Accepted Manuscript

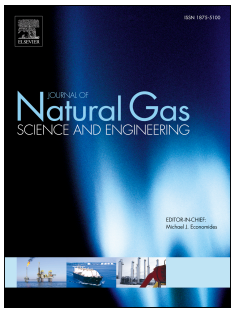

A study into the effect of cleat demineralisation by hydrochloric acid on the permeability of coal

Luc G. Turner, Karen M. Steel

PII: S1875-5100(16)30805-8

DOI: 10.1016/j.jngse.2016.11.003

Reference: JNGSE 1913

To appear in: *Journal of Natural Gas Science and Engineering*

Received Date: 27 June 2016

Revised Date: 28 October 2016

Accepted Date: 2 November 2016

Please cite this article as: Turner, L.G., Steel, K.M., A study into the effect of cleat demineralisation by hydrochloric acid on the permeability of coal, *Journal of Natural Gas Science & Engineering* (2016), doi: 10.1016/j.jngse.2016.11.003.

A study into the effect of cleat demineralisation by hydrochloric acid on the permeability of coal

Luc G. Turner and Karen M. Steel*
School of Chemical Engineering, University of Queensland, St Lucia, 4072, Australia
*Corresponding author. Email: karen.steel@uq.edu.au

Abstract

Mineral occlusions in cleats are known to considerably reduce coal permeability. Sequential steady state core flooding experiments with aqueous hydrochloric acid (HCl) solutions were conducted on whole core samples from the Bowen Basin, Australia, to assess the effect of mineral dissolution on core permeability. Cleat minerals were characterised by scanning electron microscopy with energy dispersive x-ray spectroscopy (SEM-EDS). Generally, the cleats contained kaolinite and carbonates which were present in various proportions as either single phases or mixed. An immediate increase in permeability was obtained after HCl was flooded through for the majority of tests. This increase coincided with heightened concentrations of Ca and Fe in the effluent and is attributed to the dissolution of acid soluble minerals, mainly calcite and siderite. In some cases the increase in permeability was very high (200 times increase) and sustained whilst in other cases there was a gradual decrease after the initial increase, resulting in either a small overall increase in permeability of about 20-30% or a decline in permeability relative to the original level of about 20-30%. A possible reason for permeability decline is that although dissolution of minerals allows more liquid into the core, it is not enhancing flow paths, i.e. restrictions to flow in the cleats still exist. Another reason could be destabilisation of insoluble minerals, causing them to become mobile fines in the liquid which migrate toward restrictions in the flow and then jam. High and sustained permeability increases are attributed to cleats containing solely calcite in addition to having high connectivity. This investigation has shown that cleat demineralisation using HCl can be an effective means to overcome low permeability provided cleat connectivity and mineralogy are characterised.

1 Introduction

Since 1996, the production of gas from eastern Australia has risen from 1 PJ to around 457 PJ/a in 2014-15 (DNRM, 2016). The majority of the gas will be exported to meet the strong global demand for LNG. Assuming a coal deposit contains gas, the key determinant for the rate of productivity from that deposit is the permeability of the coal, and the natural cleat system in the coal plays the primary

role in dictating permeability (Flores, 2014). If permeability is low, the most common intervention applied to coal seams is hydraulic fracturing which involves injecting a fluid containing sand particles into the formation at high pressure in order to cause the formation to crack and to deliver sand into the cracks. The fluid flows back and the sand acts as "proppants" that keep the newly formed fractures open. The fluid itself can be solely water or can contain a variety of chemicals aimed at structuring the fluid and assisting delivery of the sand (King, 2012).

There were early signs that hydraulic fracturing using gel-based fluids was problematic for coal. Traditionally, fluids would be laden with a linear gel such as guar. Puri et al. (1991) observed a substantial and irreversible decrease in permeability when coal was treated with these gels. The reason was considered to be sorption induced swelling of the coal matrix and possibly also plugging of the cleats. Other chemicals, in particular surfactants, were found to be particularly detrimental. A concern when fracture stimulating a coal seam is doing irreversible damage to the flow paths. High stress, cleating and low Young's Modulus in coal can lead to complex and inefficient fractures compared to conventional reservoirs (Olsen et al., 2007). The creation and transport of fines due to shear failure can reduce the frac conductivity and thus coal permeability. Shear failure of coal during horizontal completions can lead to reduced well productivity due to reduced permeability and fines generation (Palmer et al., 2005). Any stimulation method must try to retain the structural integrity of the formation and ensure flow paths remain open.

The natural cleat system that exists in coal could provide a ready-made opportunity for increasing permeability. Recent investigations have discussed the use of graded proppant injection for stimulation of the cleat network (Khanna et al., 2013, Keshavarz et al., 2014). Low permeability in coal seams has often been attributed to the presence of highly mineralised cleats which may occlude fracture porosity (Laubach et al., 1998, Faraj et al., 1996, Han et al., 2010, Dawson and Esterle, 2010). Cleat de-mineralisation by acids may lead to an increase in cleat connectivity and/or the creation of additional flow channels that lead to an overall increase in permeability (Turner et al., 2013).

There have been many studies on the use of acidisation treatments to enhance the permeability of conventional sandstone and carbonate reservoirs via matrix acidisation (Hartman et al., 2003, Buijse et al., 2004, Alkhaldi et al., 2010, Fredd and Fogler, 1998), though applications specific to coal permeability enhancement are limited. Vasyuchkov (1985) studied the influence of aqueous HCl (2, 4 and 6%) solutions on the permeability of coal under varied hydrostatic loading conditions. Permeability enhancement from less than 0.1 mD to over 15.1 mD was observed during flooding with 6% HCl and permeability increase was similar regardless of HCl concentration. Enever et al. (1994) examined the effect of HCl on heavily mineralised coal core samples and found highly variable results with the majority of samples showing an increase ranging from 2 - 1265 times the original permeability, though permeability reduction was also observed.

This paper attempts to elucidate the physical and chemical mechanisms occurring when coal cores from the Bowen Basin are treated with HCl in core flooding experiments and, consequently, identify situations leading to increases (or decreases) in permeability. The intention is for the acid to treat the near wellbore region and surrounding cleat structure to allow a greater flow rate of gas from the outer regions which have not been affected by acid treatment. Therefore, the acid is not expected to come into contact with the vast majority of where methane is held and therefore not influence methane desorption directly. The acid treatment may alter the surface properties of the coal and therefore influence relative permeability behaviour, however, this is expected to be vastly overridden by a substantial increase in permeability afforded by removal of minerals within cleats.

2 Experimental

2.1 Core sampling and preparation

A variety of cores from the central and southern Bowen Basin (Australia) were obtained from vertically orientated wells. The core samples were immediately vacuum sealed and stored at 4°C prior to inspection. A number of sub-samples were selected from each whole core sample for core flooding experiments. Sections (> 50 mm length) were broken parallel to the bedding plane and encapsulated in a flexible polyurethane resin approximately 3 mm thick using a custom manufactured Teflon mould. Parallel core ends were formed by hand-sanding. This mounting procedure filled in surface fractures and provided a smooth surface for application of radial confining pressure within the Hassler core holder and also prevented fluid leakage. Bulk volume was measured by liquid displacement prior to polyurethane encapsulation. Pore volume (PV) was measured by vacuum saturation in 4% KCl for 48 hours. Porosity (ϕ) was then calculated by dividing PV by bulk volume. Additional properties of core samples used are summarised in Table 1.

Table 1. Properties of core flooding samples.

Well	Sample	Depth (m)	D (mm)	L (mm)	ϕ (%)
A	A1	Pit-mined	75.20	72.78	10.47
	A2	Pit-mined	75.20	68.89	9.41
	A3	Pit-mined	75.20	77.81	5.33
B	B1	1247.04	76.20	81.81	2.34
	B2	1246.96	76.20	60.55	3.28
	B3	1249.83	76.20	79.81	2.65
C	C1	1272.02	76.20	76.37	8.46
	C2	1272.12	76.20	72.00	6.47
	C3	1287.82	76.20	74.96	4.62
	C4	1287.88	76.20	63.34	4.16
D	D1	288.76	76.20	79.04	13.32

2.2 Cleat mineralogy characterisation

Scanning electron microscopy and energy dispersive spectroscopy (SEM-EDS) was used to determine the relative abundance of cleat minerals in core flooding samples. Cleat minerals were carefully flaked out from core samples using a scalpel and mounted on 12.6 mm diameter pin type mounts with carbon tabs. A low-vacuum JEOL6460LA environmental SEM with EDS was utilised for all analyses. Backscatter electron (BSE) images were taken from regions of interest, where grayscale intensity variation indicated different elemental composition. Minerals were then identified according to their EDS spectra and atomic percentage to form a semi-quantitative cleat mineral survey for each core sample.

2.3 Core flooding experiments

The core flooding rig setup utilised for permeability measurements is shown in Figure 1. The primary components include a high pressure Quizix QX6000 pump (Chandler Engineering) for pore pressure control, a Hassler core holder (Core Laboratories), an Enerpac P-141 hand pump for confining pressure control and Equilibar back pressure regulator for outlet pore pressure control. Vacuum saturated cores were mounted inside the Hassler core holder and radial confining pressure (σ_c) was increased to 20 bar. Inlet pore pressure (P_1) and outlet pore pressure (P_2) were set at 10 bar and 8 bar respectively, thereby maintaining a constant pressure drop of 2 bar and an effective stress (σ_e) of approximately 11 bar, whereby σ_e is calculated by:

$$\sigma_e = \sigma_c - \left(\frac{P_1 + P_2}{2}\right) \tag{1}$$

Permeability was calculated by Darcy's Law:

$$k = \frac{4Q_0\mu L}{\pi D^2(P_1 - P_2)} \tag{2}$$

where Q_0 is the liquid flow rate, μ is viscosity, L is core length and D is core diameter. The constant effective stress was necessary to prevent fluid leakage around the core circumference during flooding. As minerals dissolve from within the cleats this effective stress could be sufficient to cause parts of the coal matrix to move into the volume that has been created from the mineral dissolution, and therefore alter the cleat network arrangement. The propensity for this to happen may depend on the configuration of the cleat network. The liquid flow rate will change as changes occur to the sample during acid treatment, and a change in liquid flow rate will register as a change in permeability, i.e. if liquid flow rate increases, permeability increases. The permeability is therefore a bulk property of the core. Instead of recording the permeability as a function of time, it was recorded as a function of the

number of pore volumes to pass through the core, where pore volume (PV) has the unit of ml. The environment temperature for all experiments was ambient at 22°C.

Sequential core floods with 4% KCl followed by 1% HCl/4% KCl (hereafter known as KCl and HCl respectively) were completed to obtain k_0 and k_1 respectively, and a permeability enhancement factor calculated by k_1/k_0. A background concentration of 4% KCl was used in the HCl stimulation fluid in order to prevent (or greatly reduce) the influence of clay swelling (Chen et al., 2013). Fluid switchover from KCl to HCl occurred when KCl permeability had reached steady state, defined by a permeability change of less than 1% over 1 PV. Liquid samples were regularly extracted from the core holder outlet and analysed via inductively coupled plasma optical emission spectroscopy (ICP-OES) with a Varian Vista Pro to determine the extent of de-mineralisation versus number of pore volumes. Only the major metal ions were included in the core flooding graphs displayed in the results section. For samples where on-line sampling of the core holder outlet was not available, elemental concentration of the final effluent solution following both KCl and HCl floods was instead reported.

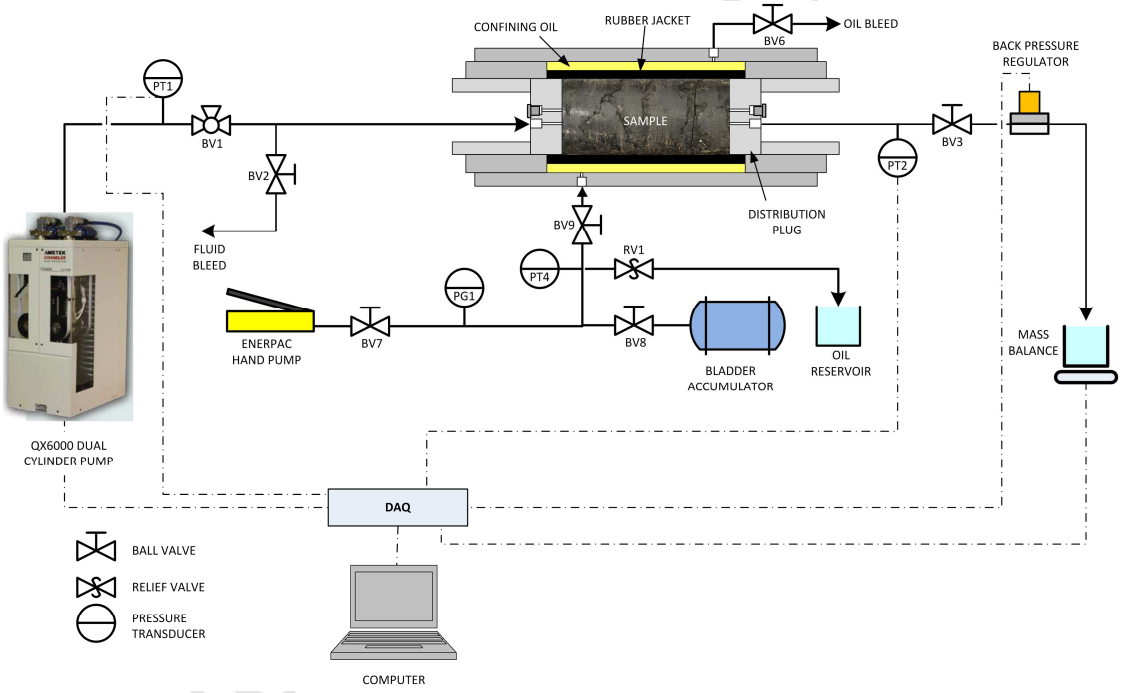

Figure 1. Core flooding rig.

3 Results

3.1 Cleat mineralogy

A summary of the major, moderate and minor/trace cleat mineralisation types found in each core is shown in Table 2. Major corresponds to minerals that are the dominant phases in the cleats. Moderate corresponds to minerals that are significant but not dominant and minor/trace corresponds to minerals that are present in small quantities. These measures are to be used as a guide given only a limited

number of samples were taken. In addition, samples were only taken from the exterior surfaces and may not fully reflect the minerals within. Variable quantities of clays, carbonates, sulphates, phosphates and oxides were observed including: kaolinite ($Al_2Si_2O_5(OH)_4$), illite/smectite, pyrite (FeS_2), apatite ($Ca_5(PO_4)_3(F,Cl,OH)$), anatase (TiO_2), ankerite ($Ca(Fe,Mg,Mn)(CO_3)_2$), siderite ($FeCO_3$), calcite ($CaCO_3$) and barite ($BaSO_4$). Figure 2 displays the four types of cleat mineralisation morphologies observed in SEM images, including: (a) mixed layer clay and carbonates; (b) single large aperture (> 100 µm) calcite or barite filled fractures; (c) clay dominant cleats with minor carbonate or barite phases; (d) mixed layer clays. Figure 3 shows SEM images of the minerals taken from the cores.

Table 2. Relative abundances of minerals observed within the cleats or primary fractures of core samples.

Sample	Majors	Moderates	Trace
A1	Kaolinite	Pyrite	Apatite, Anatase
A2	Kaolinite	Pyrite	Apatite, Anatase
A3	Kaolinite	Pyrite	Apatite, Anatase
B1	Kaolinite	(-)	Sulphate (Ca, Fe, Mg)
B2	Kaolinite	(-)	Sulphate (Ca, Fe, Mg)
B3	Kaolinite, Illite	Ankerite, Siderite	Anatase
C1	Kaolinite, Calcite	Smectite (K)	Illite (K)
C2	Calcite, Barite	Illite (K), Kaolinite	Smectite (K)
C3	Calcite, Barite	Illite (K), Smectite (K)	Barite
C4	Calcite, Barite	Illite (K), Kaolinite	Smectite (K)
D1	Illite (Fe)	(-)	Siderite

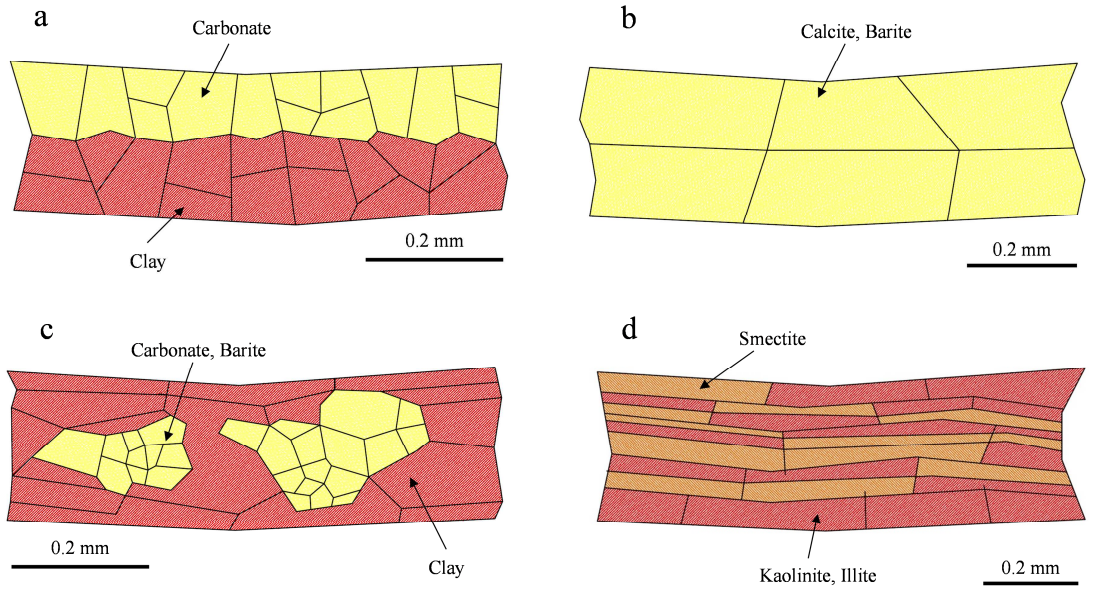

Figure 2. Cleat mineralisation morphologies observed in core samples, (a) Mixed-layered carbonate and clays; (b) Whole calcite or barite; (c) Minor carbonates and barite mixed with dominant clay; (d) Mixed-layered kaolinite, smectite and illite clays.

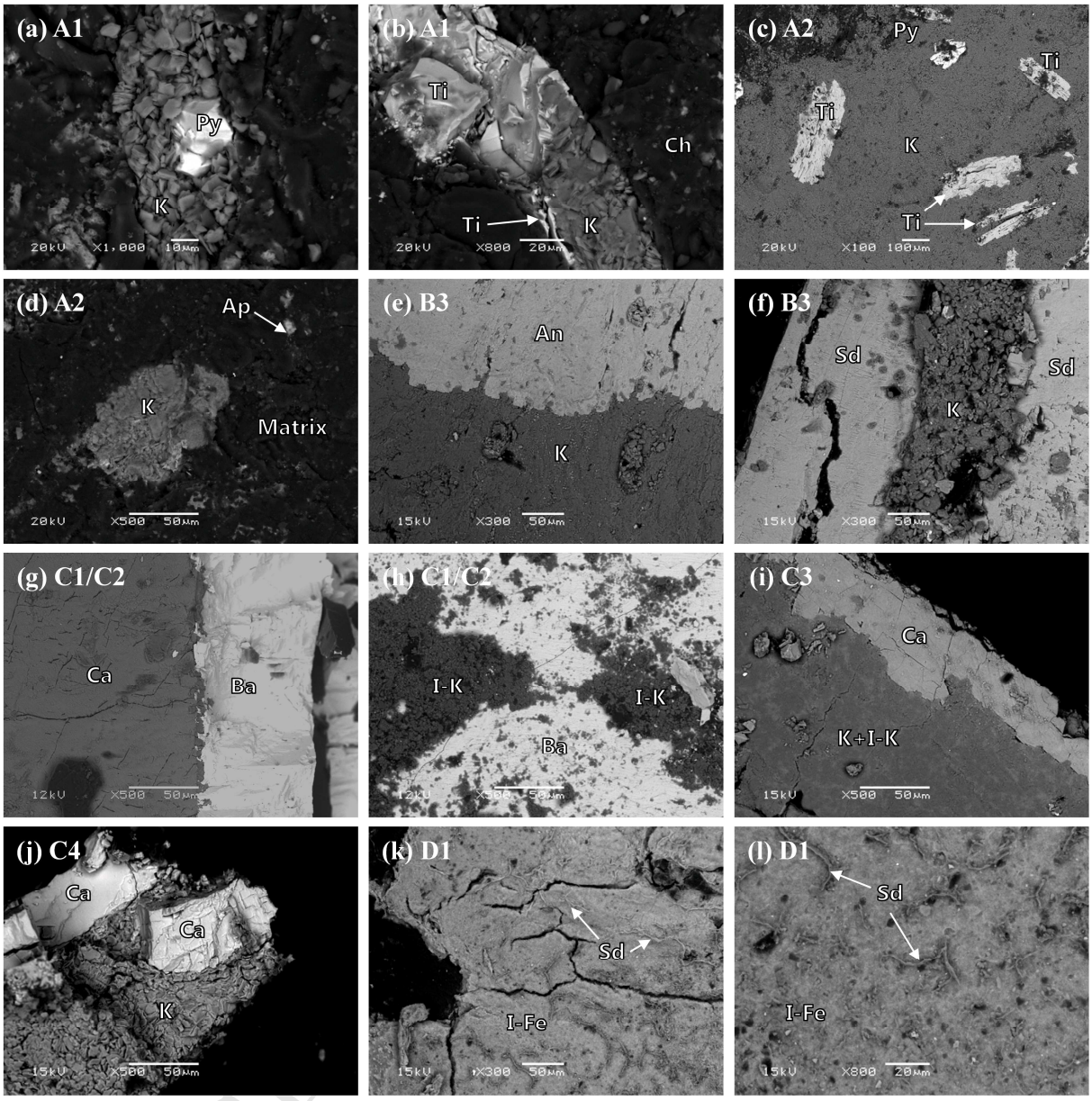

Figure 3. Backscatter electron SEM images of core and matrix mineralogy, (a) pyrite crystals (Py) in kaolinite (K) mineralised cleat (A1); (b) kaolinite (K) filled cleat with anatase (Ti) impurities and minor chlorite (Ch) matrix mineralization (A1); (c) kaolinite (K) platelet with embedded anatase (Ti) and pyrite (Py) (A2); (d) kaolinite (K) and minor apatite (Ap) matrix mineralization (A2); (e) mixed layer kaolinite (K) and ankerite (An) (B3); (f) mixed layer siderite and kaolinite (B3); (g) mixed layer calcite and barite (C1/C2); (h) mixed layer illite (K) (I-K) and barite (Ba) (C1/C2); (i) mixed layer calcite (Ca) and kaolinite (K)/illite (I-K) (C3); (j) calcite (Ca) and kaolinite (K) cleat mineralization (C4); (k) illite (Fe) (I-Fe) and minor siderite (Sd) veinlets (D1); (l) increased magnification of region highlighted in (k) (D1).

The cleat mineralogy in samples A1-A3 was kaolinite dominant mixed with moderate levels of pyrite and minor levels of apatite and anatase. Pyrite was present as a distinct phase of varying size embedded between kaolinite platelets (Figure 3a and 3c). Similar anatase morphologies were also

observed (Figure 3b and 3c). Apatite was detected in the matrix of the coal rather than in the cleat mineralogy (Figure 3d).

Sample B3 contained mixed-layered kaolinite and ankerite/siderite. The ankerite/siderite was observed as clearly defined layers adjacent to the kaolinite platelets (Figure 3e and 3f). The dominant cation (Fe-Ca-Mg) within the ankerite carbonates varied considerably.

Samples C1 and C2 were adjacent samples. The exposed core surface following breakage of C1 and C2 samples revealed multiple cleat orientations. Large aperture cleats containing predominantly calcite and minor barite were identified. Smaller cleats containing mixed-layered calcite and barite, and mixed barite and illite (K) were also identified (Figure 3g and 3h). Samples C3 and C4 were adjacent samples taken from a deeper section of the well. Cleats in C3 were clay dominant and contained varying quantities of mixed-layered kaolinite and illite. Mixed-layered kaolinite/illite (K) and calcite was also observed (Figure 3i). Photographs of the exposed inlet and outlet face of C4 are shown in Figure 4. A major cleat in C4 was calcite filled and also contained minor kaolinite (Figure 3j). This cleat ran at right angles to many other cleats at the inlet that were predominantly composed of mixed-layered illite (K)/smectite and trace barite. Other fractures were barite filled only.

D1 contained few cleats and those that were visible were only sporadically mineralised with illite (Fe) containing minor siderite veinlets, as shown in Figure 3k and 3l.

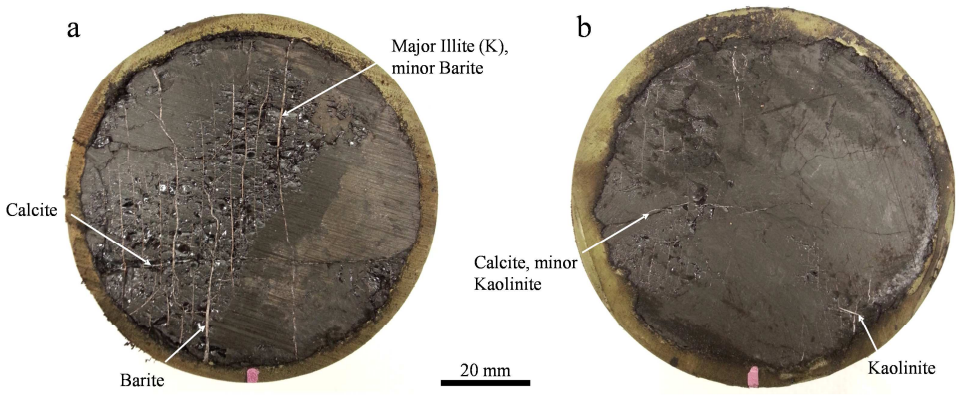

Figure 4. Photographs of C4: (a) core inlet and (b) core outlet.

3.2 Core flooding experiments

A summary of the experimental results is shown in Table 3. The experimental data for each core flood is presented and described in the following sections. In-situ liquid analysis of the effluent solution during KCl and HCl floods is also included. This is followed by a discussion of the mechanisms controlling permeability change.

Table 3. Summary of core permeability after KCl (k_0) and HCl floods (k_1)

Sample	k_0 (mD)	k_1 (mD)	k_1/k_0
A1	0.7154	0.6026	0.84
A2	1.1748	0.9935	0.85
A3	0.0456	0.0358	0.79
B1	0.1050	0.1282	1.22
B2	0.6539	0.7940	1.21
B3	0.0056	0.0042	0.75
C1	0.0955	0.2220	2.32
C2	0.0296	0.0198	0.67
C3	0.3819	0.4731	1.24
C4	0.2718	56.25	206.95
D1	0.8581	0.9477	1.10

3.2.1 A1 – A3

Figure 5 shows the permeability vs number of PVs injected during core flooding of A1 using 4% KCl followed by a mixture of 1% HCl/4% KCl. Permeability stabilises at approximately 0.72 mD using KCl. When HCl is injected there is an initial abrupt increase and decrease before reaching a peak just above 0.75 mD. The peak corresponds to the presence of Ca and P in the effluent. This suggests that the apatite is dissolving. Following the peak, permeability progressively declines to 0.60 mD such that the calculated k_1/k_0 was 0.84, or a 16% decrease in permeability. The decline in permeability matches the decline in concentration of Ca and P in the effluent, however, the concentrations of Al and Si in the effluent increases over the same period (Figure 6), suggesting that some of the kaolinite dissolves. The initial abrupt increase and decrease in permeability upon injection of HCl was due to entrainment of air within the inlet fluid line during fluid switchover.

The steady state KCl permeability for A2 was approximately 1.2 mD (Figure 7). Following injection of HCl the permeability initially increased slightly but then gradually decreased to approximately 1.0 mD, a 15% decrease from the original value. This result is similar to that found for A1. Dissolved elemental concentrations in the outlet solution following the complete KCl and complete HCl floods are shown in Table 4. There is an increase in the levels of Ca, Fe, Mg, Na, P and S. Again, this suggests that apatite is dissolving. The levels of Al and Si in the final effluent are not high. It is not known what the levels were during flooding.

The permeability of A3 in KCl was very low and stabilised at approximately 0.046 mD (Figure 8). Permeability immediately declined during HCl injection, reaching a plateau of approximately 0.036 mD with increased HCl injection. Overall calculated k_1/k_0 was then 0.79. Table 4 shows an increase in the levels of Al, Ca, Fe, Mg, P and Si. This result is similar to that found for A1 and A2, suggesting that dissolution of both acid soluble minerals and kaolinite is occurring.

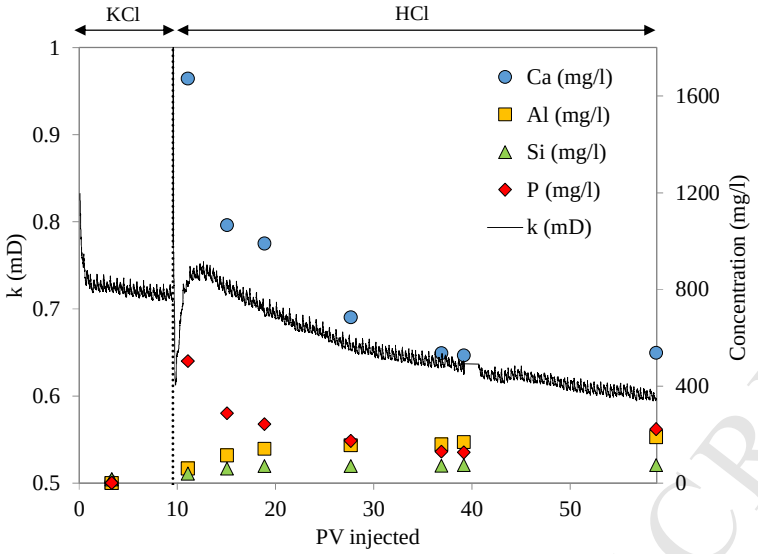

Figure 5. Permeability change of A1 during flooding with 4% KCl and 1% HCl/4% KCl.

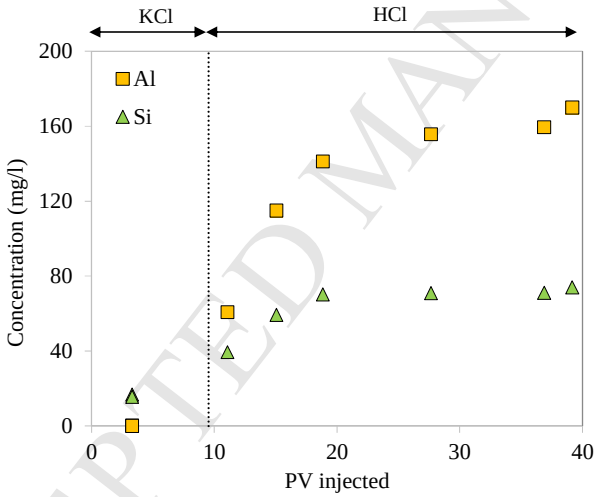

Figure 6. Al and Si concentration during flooding of core A1 with 4% KCl and 1% HCl/4% KCl.

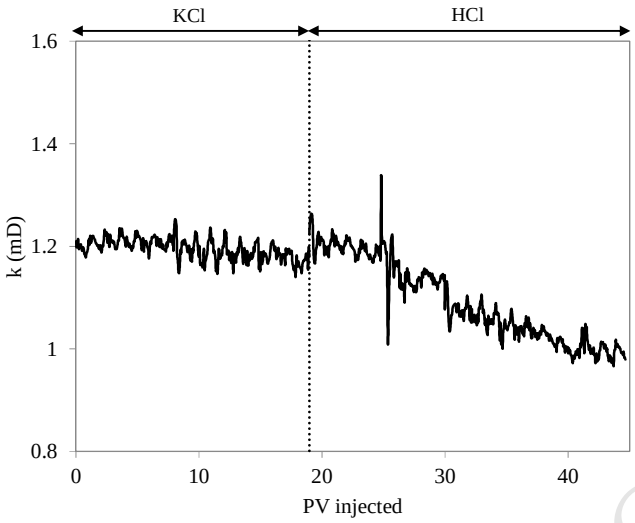

Figure 7. Permeability change of A2 during flooding with 4% KCl and 1% HCl/4% KCl.

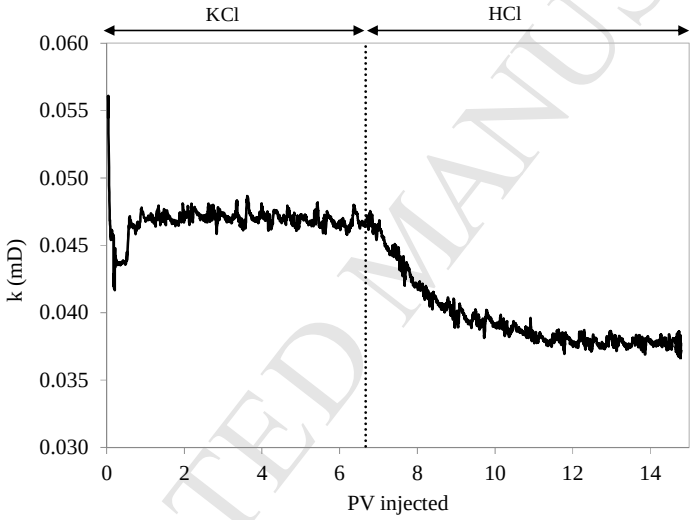

Figure 8. Permeability change of A3 during flooding with 4% KCl and 1% HCl/4% KCl.

Table 4. Elemental concentration (mg/l) pre and post HCl flooding of A2 and A3.

Core	Pre/Post	Al	Ba	Ca	Fe	K	Mg	Mn	Na	P	S	Si
A2	Pre	11	0	129	23	19047	13	0	11	1	3	5
	Post	12	0	226	79	18631	24	1	24	131	23	10
A3	Pre	18	0	139	7	20820	34	1	146	0	48	17
	Post	307	1	1086	519	21527	51	2	27	374	15	161

3.2.2 B1 – B3

The permeability of B1 using KCl reached a steady state value of approximately 0.11 mD (Figure 9). Upon injection of HCl, there was a spike in the concentration of Ca, Fe and Mg in the effluent and

permeability gradually increased to a maximum of 0.14 mD. The concentration of these elements in the effluent decreased with increasing HCl injection. The permeability also decreased slightly to 0.13 mD, giving an overall permeability increase (k_1/k_0 of 1.22). The levels of Al and Si in the final effluent were low at 5 and 13 mg/l, respectively. Although not detected by SEM-EDS, it is likely that ankerite was present in the core samples and dissolved.

Permeability for B2 was initially 0.65 mD and, similarly to B1, increased gradually to a peak value of approximately 0.79 mD during HCl injection (Figure 10). A spike in Ca concentration in the effluent corresponded to the increase in permeability. In this case there was no observed decline in permeability. Given the high concentration of Ca recorded (1200 mg/l), it is strongly suspected that calcite is present in the sample and that it dissolves. Although carbonate minerals were not found on the surface of B2, they were found on sample B3, which was taken from a few metres lower than B2. k_1/k_0 for B2 was similar to B1 at 1.21. The levels of Al and Si in the final effluent were low at 5 and 4 mg/l, respectively.

The permeability for B3 was considerably lower than that observed for other cores (Figure 11). Permeability with respect to KCl was approximately 0.006 mD and increased to a peak of 0.007 mD after HCl injection, before gradually decreasing to 0.004 mD. Dissolved elemental concentrations in the outlet solution following KCl and HCl floods is shown in Table 5. An increase in Al, Ca, Fe, Mg and Si was observed, which suggests that the carbonates are dissolving and the kaolinite also appears to be dissolving to an extent.

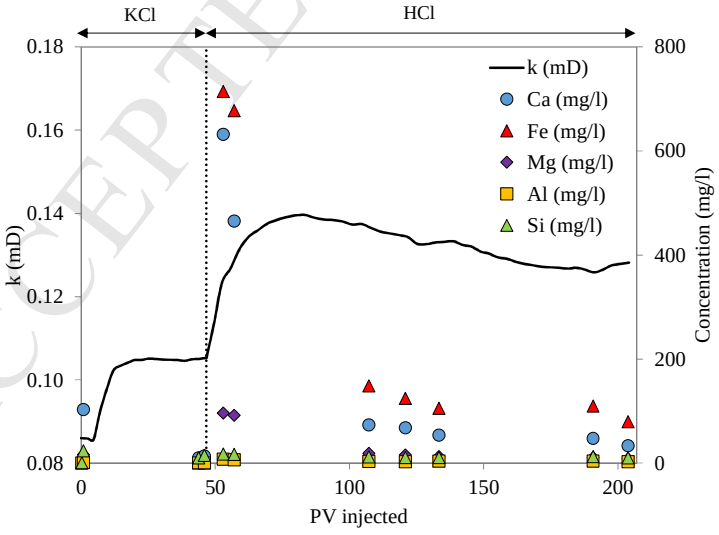

Figure 9. Permeability change of B1 during flooding with 4% KCl and 1% HCl/4% KCl.

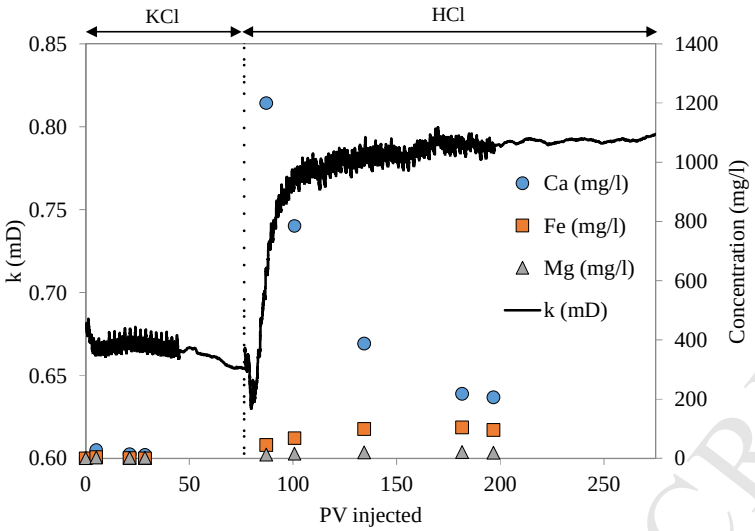

Figure 10. Permeability change of B2 during flooding with 4% KCl and 1% HCl/4% KCl.

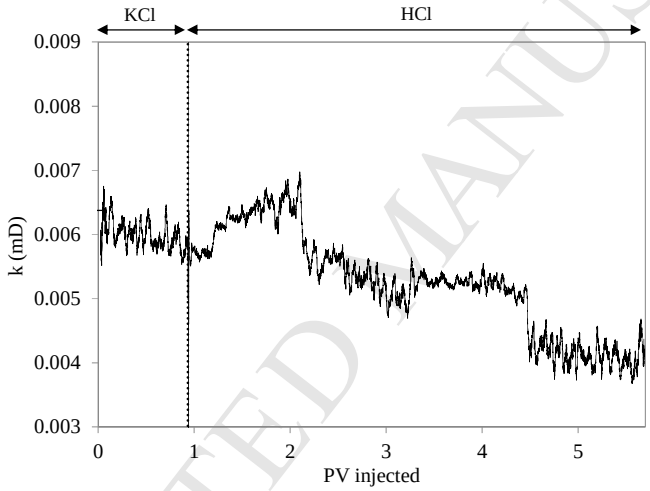

Figure 11. Permeability change of B3 during flooding with 4% KCl and 1% HCl/4% KCl.

Table 5. Elemental concentration (mg/l) pre and post HCl flooding of B3.

Pre/Post	Al	Ba	Ca	Fe	K	Mg	Mn	Na	P	S	Si
Pre	0	60	81	0	20448	20	0	1332	0	3	3
Post	32	51	117	922	20222	102	4	517	0	1	52

3.2.3 C1 – C4

Permeability reached a steady state value of approximately 0.096 mD during KCl flooding of C1 (Figure 12). Permeability response during HCl injection of C1 was characterised by step-change increases, plateau periods, and gradual increases. The final recorded permeability was 0.222 mD, and therefore k_1/k_0 was 2.32. The step-change increase in permeability coincides with a large amount of Ca in the effluent (maximum 6770 mg/l). Calcite was found to be a dominant mineral in the cleats and

was found to be present on its own in some cleats. Photographs of the core inlet surface before and after HCl flooding are shown in Figure 13. The regions of calcite dissolution are shown by the red arrows. Cleat minerals that had not dissolved were extracted from three separate regions and analysed by SEM-EDS. The minerals in regions 1 and 2 contained barite and minor illite (K), whilst region 3 contained mixed-layered barite and kaolinite. The levels of Al and Si in the final effluent were approximately 3 mg/l.

The permeability of C2 was 0.030 mD (Figure 14) and therefore considerably lower than that for C1 despite these samples being adjacent (Table 1). Permeability immediately increased during HCl injection and reached a maximum of 0.037 mD. This maximum coincided with 3000 mg/l Ca in the effluent. Further injection of HCl resulted in a progressive decrease in permeability to a plateau of 0.020 mD and there was a reduction in the amount of Ca in the effluent. Ba, which is known to be present in the sample as barite did not dissolve appreciably during HCl injection. Photographs of the core inlet and outlet surface of C2 before and after HCl flooding are shown in Figure 15. The extensive calcite mineralisation visible prior to HCl flooding (Figure 15a) appears to have dissolved (Figure 15b). The undissolved minerals following HCl flooding were extracted from separate regions at the core inlet (Figure 15b) and core outlet (Figure 15c) and analysed via SEM-EDS. Undissolved cleat minerals from region 1 in the core inlet contained a mixture of illite (K), barite and anatase phases, whereas region 2 in the core outlet contained predominantly barite. Al and Si concentrations in the final effluent increased slightly during HCl flooding to approximately 30 mg/l and 22 mg/l, respectively (Figure 16). Fe also increased up to a maximum of 153 mg/l before decreasing slightly to 132 mg/l when flooding was terminated.

C3 had a higher permeability than C1 and C2 during KCl injection of approximately 0.38 mD (Figure 17). Permeability increased sharply to a peak value of 1.26 mD before declining steadily to 0.47 mD upon continued injection of HCl. As with other samples the increase in permeability coincided with high levels of Ca in the effluent (max 3169 mg/l). The levels of Al and Si in the final effluent were only 3 and 5 mg/l, respectively.

C4 had a permeability of approximately 0.27 mD during KCl injection (Figure 18). Following HCl injection the permeability increased rapidly and reached a peak of 56 mD. As with the other samples, the permeability did decrease, but only to 44 mD. This gave a final calculated k_1/k_0 of 207. This was significantly larger than all other samples. Permeability increase coincided with an increase in Ca in the effluent (maximum 1943 mg/l). The levels of Al and Si in the final effluent were 3 and 5 mg/l, respectively. It is interesting that the behaviours of C3 and C4 during HCl injection should be so different given that they are adjacent samples. It is also worthwhile to note that despite the large permeability increase in C4, permeability decline is still observed following prolonged HCl injection. This suggests that the mechanism for permeability decline is also occurring here.

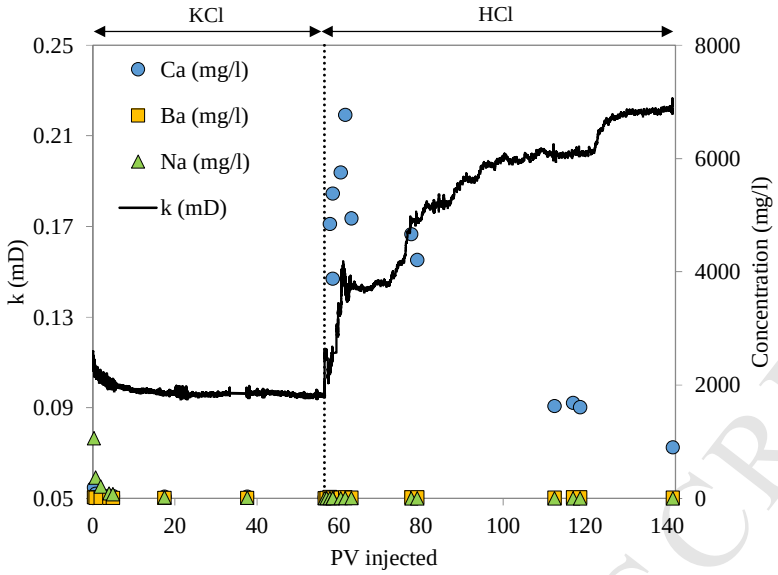

Figure 12. Permeability change of C1 during flooding with 4% KCl and 1% HCl/4% KCl.

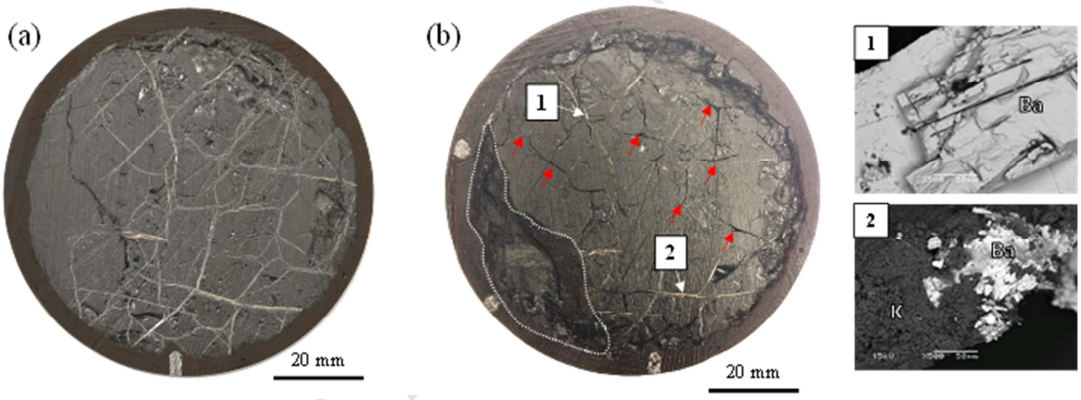

Figure 13. Photographs of C1 inlet, (a) before HCl flood, and (b) after HCl flood, where red arrows highlight regions of calcite dissolution. The white dotted area highlights core breakage following removal from the core holder assembly. SEM images of cleat minerals extracted from regions (1) and (2) in (b) are also shown, where Ba = barite and K = kaolinite.

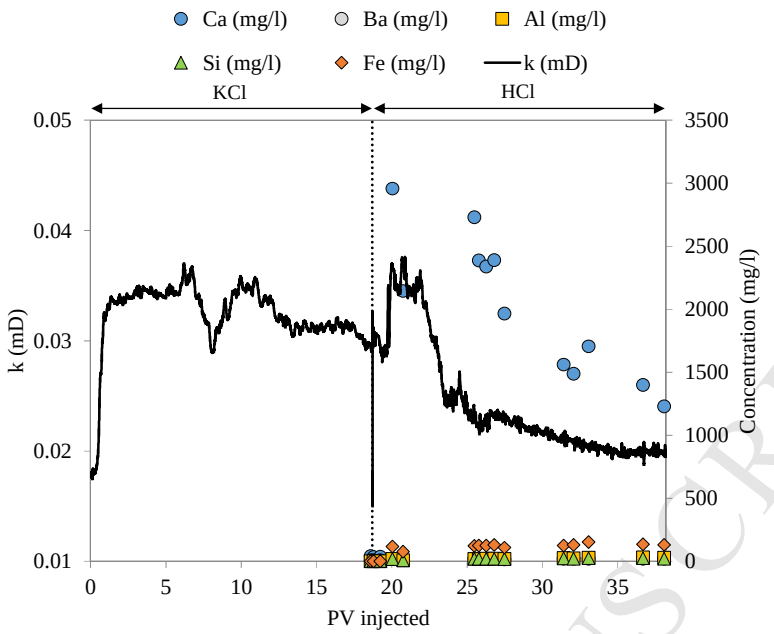

Figure 14. Permeability change of C2 during flooding with 4% KCl and 1% HCl/4% KCl.

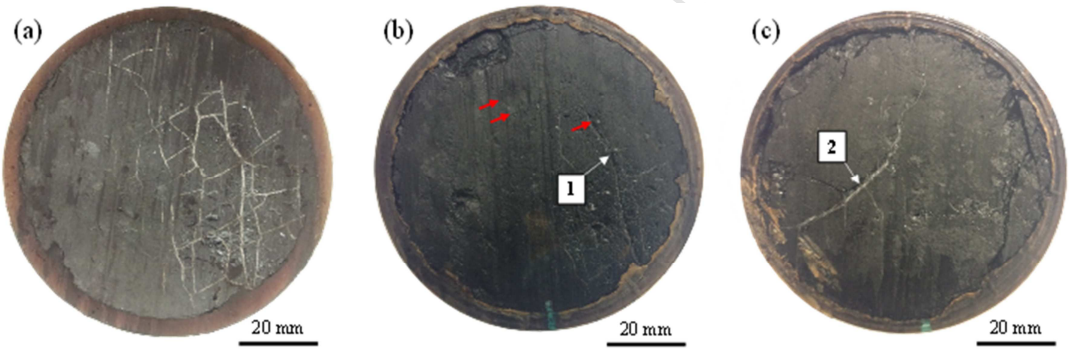

Figure 15. Images of C2, (a) core inlet prior to HCl flood; (b) core inlet after HCl flood, where red arrows highlight de-mineralised cleats and region 1 contained barite, illite (K) and anatase; (c) core outlet after HCl flood, where region 2 contained barite.

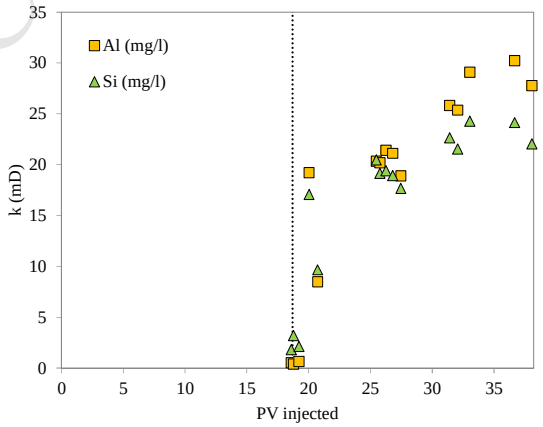

Figure 16. Al and Si concentration during flooding of C2 with 4% KCl and 1% HCl/4% KCl.

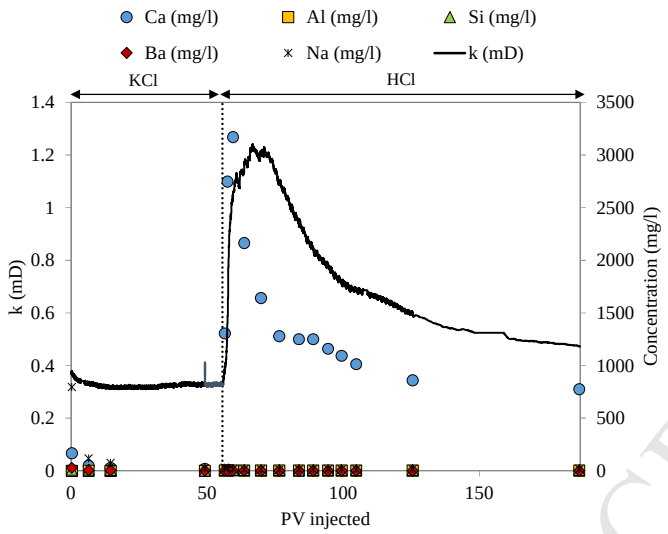

Figure 17. Permeability change of C3 during flooding with 4% KCl and 1% HCl/4% KCl.

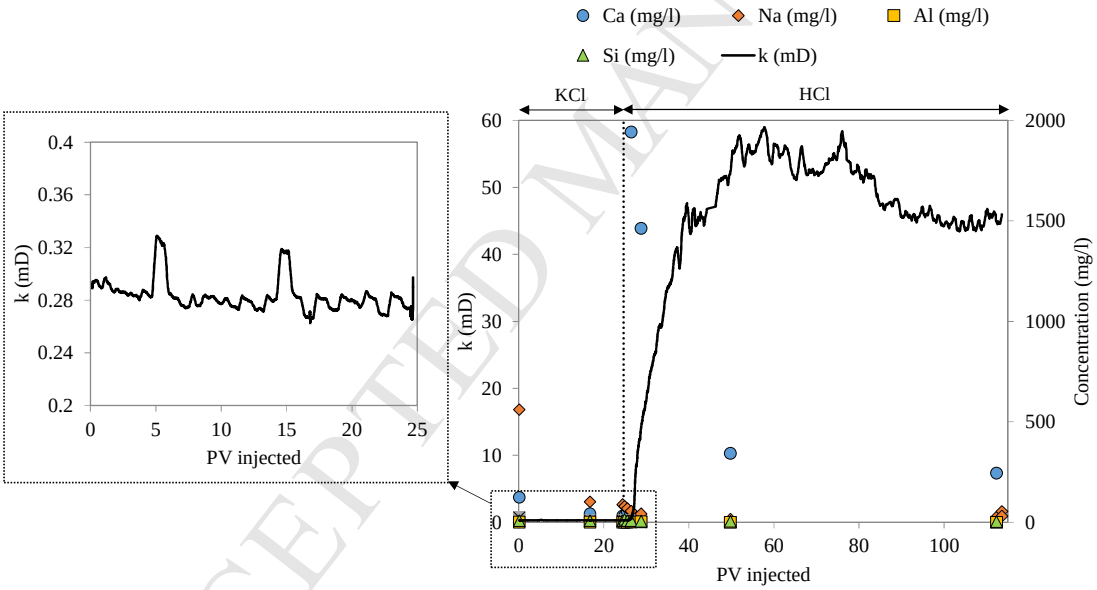

Figure 18. Permeability change of C4 during flooding with 4% KCl and 1% HCl/4% KCl, (a) magnification of 4% KCl flooding stage, and (b) 4% KCl and 1% HCl/4% KCl combined.

3.2.4 D1

The KCl permeability of D1 was 0.86 mD and increased rapidly to a maximum of 1.34 mD during HCl injection (Figure 19). Permeability then decreased gradually to 0.96 mD after further HCl injection giving a k_1/k_0 of 1.10. The mineralogy of this sample was quite different to the others and comprised Fe bearing illite that contained small veinlets of siderite. The increase in permeability coincided with an increase in Fe concentration in the effluent, however, the maximum concentration

(380 mg/l) occurred after the permeability reached a maximum. Al and Si levels stayed low and were 4 mg/l and 7 mg/l, respectively, at the end of the experiment. Release of Ca reached a maximum of only 7 mg/l.

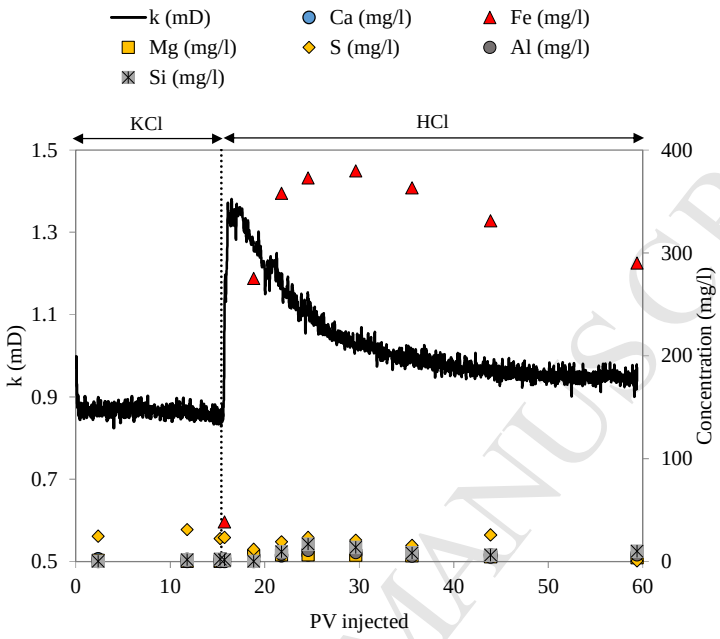

Figure 19. Permeability change of D1 during flooding with 4% KCl and 1% HCl/4% KCl.

4 Discussion

The trend of increasing permeability followed by a decline during HCl flooding suggests two competing mechanisms, the balance of which yields a peak. The height of the peak and the decline that follows the peak is dictated by how well each mechanism is able to compete with the other. The mechanism by which the permeability increases is most likely to be acid soluble minerals dissolving and allowing enhanced liquid flow. A second mechanism then competes against this to cause liquid flow to be restricted. The extent that this mechanism competes is highly variable. For some core samples the extent is minimal, while for others it is so significant that the permeability is reduced to what it was initially, or lower.

The reason why permeability did not increase for the A series of samples despite Ca being present in the effluent may be due to the apatite being located in the matrix of the coal rather than in the cleats. High concentrations of Al and Si were found in the effluent for the A series of cores which strongly suggests that kaolinite within the cleats is dissolving. One idea for the reason behind kaolinite dissolution is that when the apatite dissolves it forms weak hydrofluoric acid and that this hydrofluoric

acid reacts with the kaolinite. However, the dissolution of kaolinite did not result in an increase in permeability. Instead, the permeability declined as more HCl was flushed through the core.

The permeability decline trends for A1, A3, C3 and D1 follow a smooth trend towards a minimum, or plateau. The rate of decline is highest at the beginning and lowest at the end. Figure 5 shows that the concentration of Ca in the effluent for A1 also follows this trend whereby the rate of decline for Ca concentration is highest at the beginning and lowest at the end. The apatite is expected to react and dissolve in HCl rapidly and so the Ca trend is expected. While HCl is in excess the amount of apatite available for reaction decreases over time and so the amount of Ca in solution decreases and is expected to drop to zero when all of the available apatite has dissolved. Given that the amount of Ca in the effluent was 500 mg/l at the end of the experiment, not all of the apatite had dissolved by the end of the experiment. The trend for kaolinite dissolution is different and this is due to its slower rate of reaction. As stated above the dissolution of apatite is expected to release HF into the solution and it is reasonable to assume that released HF would react with kaolinite. Therefore, given the constant supply of HF and the slow kinetics of kaolinite dissolution the rise of Al and Si in solution is expected. As for apatite, the dissolution of kaolinite is not complete. If the experiment had continued for longer, the levels of Al and Si in the effluent are expected to have declined.

Unlike the A series, the B series of cores had significant acid soluble minerals within the cleats, in the form of ankerite which was found to be mixed with kaolinite. Considerable levels of Ca and Fe were detected in the effluent during HCl flooding. The levels of Al and Si were found to be very low in the effluent, which suggests that the kaolinite does not dissolve. For the B series, the permeability did not decline considerably for B1 and B2, which suggests that the second mechanism was not occurring to a large extent.

For the C series of cores, there were mixed results. These cores contained considerable amounts of calcite. The calcite was found to be dominant within some of the cleats and mixed with kaolinite in other cleats. For C1 there was considerable calcite dissolution, very little Al and Si dissolution, and no decline in permeability. For C2 there was considerable calcite dissolution, a rise in the concentration of Al and Si in the effluent (Figure 16), and a decline in permeability. For C3 there was considerable calcite dissolution, negligible levels of Al and Si in the effluent, and a decline in permeability. For C4, there was considerable calcite dissolution, negligible levels of Al and Si in the effluent, and only a small decline in permeability.

At this stage there are three hypotheses to explain why the permeability increases and then decreases for certain cores. The first hypothesis is that as mineral dissolution occurs the volume occupied by the liquid containing dissolved solid is less than that of the original solid and liquid combined, which is common for the dissolution of ionic solids. This would allow, at least temporarily, an accumulation or hold-up of liquid in the core which would register as an increase in liquid flow rate and hence permeability. One would expect this phenomenon to diminish as all of the acid soluble minerals

dissolve. Therefore, the trend seen could be expected, whereby the peak in permeability corresponds to the maximum rate of mineral dissolution. Ultimately, for the permeability to drop back close to its original level the mineral dissolution that is occurring is not enhancing flow through the cleat system. There are still restrictions to flow that are not altered by mineral dissolution. If liquid hold-up is the reason for the permeability trend observed, the initial spike in permeability should be considered to be an experimental artefact and not indicative of the samples true permeability. It can serve to show that mineral dissolution is occurring and that the dissolution is not providing enhanced permeability due to other restrictions in the flow. The plateau permeability should therefore be taken as the true permeability for assessing whether there has been an overall increase or decrease in permeability.

The second hypothesis is that as minerals dissolve, or partially dissolve, it causes them or surrounding minerals to break up into particles (or fines) that become mobile within the liquid. The mobilised fines may then become jammed at cleat restrictions and progressively build up, causing increased restriction to liquid flow at those points and a reduction in permeability, as displayed graphically in Figure 20. This mechanism is also likely to follow a smooth trend that parallels the rate of mineral dissolution and therefore parallels the smooth trend observed for the permeability decline. This phenomenon could help to explain why permeability declines to lower levels than the original permeability. The detachment of fines due to carbonate cement dissolution has been observed during core flooding of carbonate samples (Bacci et al., 2011, Garing et al., 2015, Luquot et al., 2014) and sandstone samples (Pudlo et al., 2015) with CO_2 saturated brine solutions. Mineral dissolution could also result in a local liquid velocity increase within the cleats which allows enhanced transport of fines and eventual blockage of cleat restrictions. This critical velocity parameter for the generation and migration of fines has been discussed elsewhere (Keshavarz et al., 2014, Bai et al., 2015, Oliveira et al., 2014).

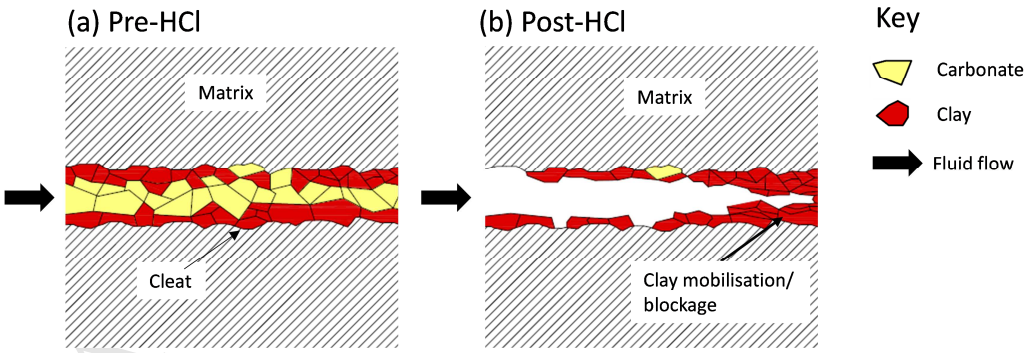

Figure 20. Graphical representation of clay fines mobilisation due to carbonate (calcite or siderite) dissolution.

The third hypothesis is that as the minerals dissolve and cause an increase in pore volume, the surrounding coal moves into that volume under the applied effective stress. This mechanism of cleat compression could also be expected to follow a smooth trend that parallels the rate of mineral

dissolution. It is important to note that this mechanism did not seem to occur for the C4 sample. Unless the cleat geometry of C4 is such that it is able to counteract cleat compression, the result for C4 suggests that cleat compression is an unlikely reason for the permeability decline and that unstable liquid flow rates due to mineral dissolution and/or fines mobilisation and jamming are more likely mechanisms.

The main recommendations for further work to better understand the mechanism(s) behind the permeability trends observed following acid stimulation are as follows:

(1) Cleat compressibility studies: Instead of obtaining a permeability at a single effective stress, obtain a stress dependant permeability both before after acid treatment. This will indicate the conditions at which cleat compression is occurring.
(2) More in-depth examination of the results using X-ray computed tomography (CT) analysis: The C3 and C4 cores are considered to be the key to understanding the permeability decline as they are adjacent to each other and have similar mineralogy, yet have a very different permeability response.
(3) Filtration of effluents followed by solids characterisation (particle size and composition). This may provide an indication of whether fines migration and jamming is occurring.

In addition, to mimic how stimulation would be conducted downhole, flooding experiments should adopt forward flow to characterise initial permeability, reverse flow with acid to simulate downhole treatment, and then forward flow again to characterise the final permeability. The reverse flow could be set up with a very small pressure drop in order to mimic the reality that mass transfer of the acid will probably be dominated by diffusion. It is recommended that the forward flow solutions mimic the downhole water chemistry in terms of salt composition, which is expected to influence the ease of mineral dissolution, and pH, which is expected to influence the amount of acid required. Studies indicate that the pH of water in the Bowen Basin is between 7 and 8 (Kinnon et al., 2010).

All experiments here have been conducted examining flow in the vertical direction. However, acid stimulation will most likely be carried out in the horizontal (flow) direction, and so experiments should be conducted on horizontal cores.

Once the mechanisms are understood it will then be necessary to examine whether there are any adverse effects with regards to relative permeability behaviour and to use the knowledge to make predictions on a larger scale, considering both the acid stimulation treatment and its effect on productivity.

5 Conclusions

This work has examined the effect on liquid permeability from flooding HCl through 11 coal cores which had various cleat and mineralogical properties. For most of the cores an increase in permeability was obtained immediately after HCl was flooded through. This increase coincided with heightened concentrations of Ca and Fe and is attributed to the dissolution of acid soluble minerals, mainly calcite and siderite. In some cases the increase in permeability was maintained while in other cases there was a gradual decrease in permeability resulting in either a small overall increase in permeability (cores C3 and D1) or a decline in permeability relative to the original level (cores A1-A3). Permeability enhancement factors therefore varied enormously from 0.79 up to 207. An increase in permeability that is sustained suggests that the mineral dissolution occurring is opening up flow paths, while a temporary increase in permeability followed by a decline suggests that while mineral dissolution is occurring it is not opening up flow paths. The precise reason why there is a peak in permeability followed by a decline may be associated with the liquid hold-up that is expected to occur during mineral dissolution and/or the dissolution of minerals destabilising insoluble surrounding minerals, causing them to become mobile in the liquid, migrate toward restrictions in the flow, and then jam. Another possible reason for the decline is that as dissolution of minerals creates additional pore volume, this volume is then compressed under the applied load on the sample. At this stage liquid hold-up and fines migration are considered to be the more likely reason as permeability decline was not found for all samples, i.e. there were samples for which minerals dissolved, additional pore volume was created and permeability stayed high, indicating that compression did not occur. This work has shown that increases in permeability can be achieved where cleats are rich in carbonates, however, the presence of clays may place limitations on the extent of enhancement. It is imperative that the cleat mineralogy and connectivity is well understood prior to implementation of a cleat de-mineralisation treatment.

Acknowledgements

The authors would like to acknowledge financial support for this work from the Centre for Coal Seam Gas at the University of Queensland. The authors acknowledge the analytical support from UQ Centre for Microscopy and Microanalysis (CMM) and The Analytical Services Laboratory at the UQ School of Agriculture and Food Sciences.

References

Alkhaldi, M. H., Nasr-El-Din, H. A. & Sarma, H. K. 2010. Kinetics of the Reaction of Citric Acid With Calcite. *SPE Journal*.

Bacci, G., Korre, A. & Durucan, S. 2011. An experimental and numerical investigation into the impact of dissolution/precipitation mechanisms on CO_2 injectivity in the wellbore and far field regions. *International Journal of Greenhouse Gas Control,* 5**,** 579-588.

Bai, T., Chen, Z., Aminossadati, S. M., Pan, Z., Liu, J. & Li, L. 2015. Characterization of coal fines generation: A micro-scale investigation. *Journal of Natural Gas Science and Engineering,* 27, Part 2**,** 862-875.

Buijse, M., Boer, P. D., Breukel, B. & Burgos, G. 2004. Organic Acids in Carbonate Acidizing. *SPE Production & Operations*.

Chen, Z., Liu, J., Elsworth, D., Pan, Z. & Wang, S. 2013. Roles of coal heterogeneity on evolution of coal permeability under unconstrained boundary conditions. *Journal of Natural Gas Science and Engineering,* 15**,** 38-52.

Dawson, G. K. W. & Esterle, J. S. 2010. Controls on coal cleat spacing. *Asia Pacific Coalbed Methane Symposium: Selected papers from the 2008 Brisbane symposium on coalbed methane and CO_2-enhanced coalbed methane,* 82**,** 213-218.

Dnrm 2016. Queensland's petroleum and coal seam gas 2014-2015. *In:* MINES, D. O. N. R. A. (ed.).

Enever, J., Gamson, P., Grace, T., Hennig, A. & Morros, O. 1994. Feasibility study to examine propsects for stimulating gas production from low permeability coal seams: Final report.

Faraj, B. S. M., Fielding, C. R. & Mackinnon, I. D. R. 1996. Cleat mineralisation of Upper Permian Baralaba/Rangal Coal Measures, Bowen Basin, Australia. *From Gayer, R. & Harris, I. (eds), Coalbed Methane and Coal Geology, Geological Society Special Publication No 109, pp 151-164*.

Flores, R. M. 2014. Coal and Coalbed Gas, Fueling the Future. *In:* FLORES, R. M. (ed.) *Coal and Coalbed Gas.* Boston: Elsevier.

Fredd, C. N. & Fogler, H. S. 1998. Alternative Stimulation Fluids and Their Impact on Carbonate Acidizing. *SPE Journal,* 3**,** 34-41-34-41.

Garing, C., Gouze, P., Kassab, M., Riva, M. & Guadagnini, A. 2015. Anti-correlated Porosity–Permeability Changes During the Dissolution of Carbonate Rocks: Experimental Evidences and Modeling. *Transport in Porous Media,* 107**,** 595-621.

Han, F., Busch, A., Krooss, B. M., Liu, Z., Van Wageningen, N. & Yang, J. 2010. Experimental Study on Fluid Transport Processes in the Cleat and Matrix Systems of Coal. *Energy & Fuels,* 24**,** 6653-6661.

Hartman, R. L., Lecerf, B., Frenier, W., Ziauddin, M. & Fogler, H. S. Acid Sensitive Aluminosilicates: Dissolution Kinetics and Fluid Selection for Matrix Stimulation Treatments. SPE European Formation Damage Conference, 2003 2003 The Hague, Netherlands. Society of Petroleum Engineers.

Keshavarz, A., Yang, Y., Badalyan, A., Johnson, R. & Bedrikovetsky, P. 2014. Laboratory-based mathematical modelling of graded proppant injection in CBM reservoirs. *International Journal of Coal Geology*.

Khanna, A., Keshavarz, A., Mobbs, K., Davis, M. & Bedrikovetsky, P. 2013. Stimulation of the natural fracture system by graded proppant injection. *Journal of Petroleum Science and Engineering,* 111**,** 71-77.

King, G. E. Hydraulic Fracturing 101: What Every Representative, Environmentalist, Regulator, Reporter, Investor, University Researcher, Neighbor and Engineer Should Know About Estimating Frac Risk and Improving Frac Performance in Unconventional Gas and Oil Wells. SPE Hydraulic Fracturing Technology Conference, 2012 2012 The Woodlands, Texas, USA. Society of Petroleum Engineers.

Kinnon, E. C. P., Golding, S. D., Boreham, C. J., Baublys, K. A. & Esterle, J. S. 2010. Stable isotope and water quality analysis of coal bed methane production waters and gases from the Bowen Basin, Australia. *International Journal of Coal Geology,* 82, 219-231.

Laubach, S. E., Marrett, R. A., Olson, J. E. & Scott, A. R. 1998. Characteristics and origins of coal cleat: A review. *International Journal of Coal Geology,* 35**,** 175-207.

Luquot, L., Roetting, T. S. & Carrera, J. 2014. Characterization of flow parameters and evidence of pore clogging during limestone dissolution experiments. *Water Resources Research,* 50**,** 6305-6321.

Oliveira, M. A., Vaz, A. S. L., Siqueira, F. D., Yang, Y., You, Z. & Bedrikovetsky, P. 2014. Slow migration of mobilised fines during flow in reservoir rocks: Laboratory study. *Journal of Petroleum Science and Engineering*.

Olsen, T. N., Bratton, T. R., Tanner, K. V., Donald, A. & Koepsell, R. Application of Indirect Fracturing for Efficient Stimulation of Coalbed Methane. Rocky Mountain Oil & Gas Technology Symposium, 2007 Denver, Colorado, U.S.A.: Society of Petroleum Engineers.

Palmer, I. D., Moschovidis, Z. A. & Cameron, J. R. Coal Failure and Consequences for Coalbed Methane Wells. SPE Annual Technical Conference and Exhibition, 2005, Dallas, Texas. Society of Petroleum Engineers.

Pudlo, D., Henkel, S., Reitenbach, V., Albrecht, D., Enzmann, F., Heister, K., Pronk, G., Ganzer, L. & Gaupp, R. 2015. The chemical dissolution and physical migration of minerals induced during CO_2 laboratory experiments: their relevance for reservoir quality. *Environmental Earth Sciences,* 73**,** 7029-7042.

Puri, R., King, G. E. & Palmer, I. D. Damage to Coal Permeability During Hydraulic Fracturing. Low Permeability Reservoirs Symposium, 1991, Denver, Colorado. Copyright 1991, Society of Petroleum Engineers, Inc.

Turner, L. G., Steel, K. M. & Pell, S. D. 2013. Novel Chemical Stimulation Techniques to Enhance Coal Permeability for Coal Seam Gas Extraction. *SPE Unconventional Resources Conference and Exhibition-Asia Pacific, 11-13 November, Brisbane, Australia.* Society of Petroleum Engineers.

Vasyuchkov, Y. F. 1985. A study of porosity, permeability, and gas release of coal as it is saturated with water and acid solutions. *Soviet Mining,* 21**,** 81-88.

Highlights:

- Permeability increases (x200) occurred for highly connected calcite dominated cleats.
- Permeability declines occurred for mixed calcite/kaolinite dominated cleats.
- Permeability declines may be due to kaolinite mobilisation and jamming.